

Enabling Rapid and Specific Surface-Enhanced Raman Scattering Immunoassay Using Nanoscaled Surface Shear Forces

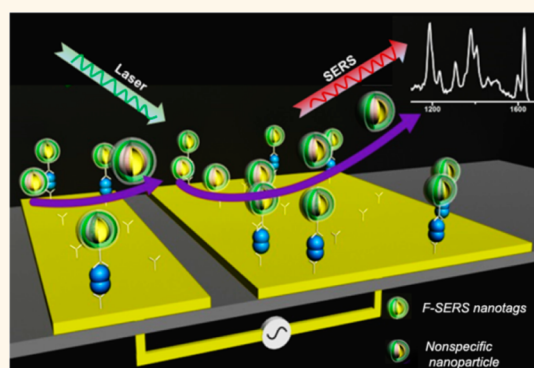
Yuling Wang,^{*,†,§} Ramanathan Vaidyanathan,^{†,§} Muhammad J. A. Shiddiky,^{*,†} and Matt Trau^{*,†,‡}

[†]Centre for Personalized Nanomedicine, Australian Institute for Bioengineering and Nanotechnology (AIBN), Corner College and Cooper Roads (Bldg 75), and

[‡]School of Chemistry and Molecular Biosciences, The University of Queensland, Brisbane QLD 4072, Australia. [§]Y.W. and R.V. contributed equally.

ABSTRACT A rapid and simple approach is presented to address two critical issues of surface-enhanced Raman scattering (SERS)-based immunoassay such as removal/avoiding nonspecific adsorption and reducing assay time. The approach demonstrated involves rationally designed fluorophore-integrated gold/silver nanoshells as SERS nanotags and utilizes alternative current electrohydrodynamic (ac-EHD)-induced nanoscaled surface shear forces to enhance the capture kinetics. The assay performance was validated in comparison with hydrodynamic flow and conventional immunoassay-based devices. These nanoscaled physical forces acting within nanometer distances from the electrode surface enabled rapid (40 min), sensitive (10 fg/mL), and highly specific detection of human epidermal growth factor receptor 2 in breast cancer patient samples.

We believe this approach presents potential for the development of rapid and sensitive SERS immunoassays for routine clinical diagnosis.



KEYWORDS: SERS · immunoassay · ac-EHD · shear force · nonspecific adsorption

Protein immunoassays have widely been recognized as a powerful analytical tool for clinical diagnosis with fluorescence and enzyme-linked immunosorbent assay (ELISA)-based assays being widely used. Recently, surface-enhanced Raman scattering (SERS) immunoassays have gained widespread interest as an effective alternative to fluorescence and ELISA-based protein assays owing to their enhanced sensitivity, multiplex capability, and photostability.^{1–3} However, the integration of SERS immunoassays for clinical diagnosis is limited by two critical problems that include (i) longer incubation periods as a result of slow binding kinetics of heavier SERS particles to the target antigen (*i.e.*, slow diffusion of particles) and (ii) high levels of nonspecific adsorption of molecules onto the sensor surface that reduce the specificity and sensitivity of detection.^{4–9} Recently, Driskell *et al.* proposed an approach to increase the flux of antigen and SERS particles to the solid-phase surface by using a

rotated capture substrate.¹⁰ The assay time was reduced from 24 h to 25 min in a 10-fold loss of sensitivity compared to the conventional SERS immunoassay. Furthermore, a syringe pump SERS immunoassay was developed to overcome diffusion-limited binding kinetics that often impedes rapid analysis in conventional SERS immunoassay.¹¹ The assay time was reduced from 24 h to 10 min with a 10-fold improvement in detection limit. Despite these attempts being successful in reducing assay times,^{10,11} nonspecific adsorption of nontarget molecules still remains the biggest challenge in immunoassays,^{12,13} in particular, SERS-based immunoassays,^{3,9} and very few attempts have been reported to address this longstanding problem. To circumvent this problem, herein, we propose an innovative platform that utilizes nanoscaled alternating current electrohydrodynamic (ac-EHD)-induced surface shear forces to enhance the capture efficiency (*i.e.*, increase diffusion of target and SERS particles) as well as

* Address correspondence to y.wang27@uq.edu.au, m.shiddiky@uq.edu.au, m.trau@uq.edu.au.

Received for review March 31, 2015 and accepted May 15, 2015.

Published online May 15, 2015
10.1021/acsnano.5b01929

© 2015 American Chemical Society

significantly reduce the nonspecific binding of molecules from the electrode surface. These surface shear forces act within nanometer distances from the electrode surface and possess the capability to induce fluid flow that can increase the number of antigen–antibody collisions while simultaneously shear away nonspecific molecules.^{14,15} Further, we believe that the use of rationally designed fluorophore-integrated gold/silver nanoshells as SERS nanotags in combination with these nanoscaled forces could represent a new effective approach to enhance the performance of SERS-based immunoassays.

To demonstrate the utility of this approach in SERS immunoassays, we constructed a multiplexed device containing an array of asymmetric electrode pairs within three individual microfluidic channels (see Experimental Methods and Figure S1 in the Supporting Information) that form the fluid control system as well as the capture domain when functionalized with an antibody. Bifunctional fluorophore-integrated gold/silver (F-SERS) nanoshells were rationally designed to demonstrate the application of ac-EHD in SERS immunoassay, which can facilitate simultaneous fluorescence and SERS measurements. These rationally designed nanoparticles consist of a gold/silver nanoshell initially coated with Raman reporters, followed by a thin layer of silica. Subsequently, fluorophore-integrated nanoshells were synthesized with an additional fluorophore coated onto a silica-coated Raman particle. The silica layer acts a protective shield between the two layers to enable both fluorescence and SERS measurements. In a typical immunoassay, the target sample and F-SERS nanoshell-tagged detection antibody were driven through the devices under the ac-EHD field. The distribution of F-SERS nanotags on the electrode surface was monitored using fluorescence microscopy, while the laser excitation on the surface resulted in quantitative target antigen detection obtained from SERS spectra with distinct fingerprints. In this study, we demonstrate the utility of nanoscaled surface shear forces for the capture and detection of human epidermal growth factor receptor 2 (HER2), an important biomarker for targeted breast cancer therapy that is overexpressed in 20–30% of breast cancer patients. HER2 overexpression is believed to be associated with a diminished prognosis (e.g., higher risk of recurrence) and may correlate with resistance to hormonal therapy and sensitivity to chemotherapy drugs. Thus, there is a need for better diagnostic methods to detect HER2 during early stages of the disease and/or to monitor disease recurrence.

RESULTS AND DISCUSSION

ac-EHD SERS Immunoassay. Figure 1a illustrates the mechanism of ac-EHD-induced surface shear forces in enhancing specificity of SERS immunocapture. The application of an alternating potential difference

across each asymmetric electrode pair results in a nonuniform field that is induced within the electrical double layer. The asymmetry in geometry results in a lateral variation in the number of charges and their spatial distribution across each electrode pair. As a result, nonuniform forces generated on the electrode surface facilitate net fluid flow with the lateral force on the larger electrode being stronger than that of the smaller electrode, thereby resulting in fluid flow toward the larger electrode. This resulting unidirectional fluid flow causes analytes in solution to be dragged by the flow and induces the necessary fluid mixing to enhance capture performance within the capture domain of the device.¹⁵ Meanwhile, these surface shear forces generated within nanometer distances (e.g., λ_D = double-layer thickness = ~ 3 – 4 nm, calculated for 1 mM phosphate buffer saline (PBS) using Debye–Hückel approximation¹⁶) from the electrode surface and its associated fluid mixing can also displace weakly bound species, thereby resulting in specific target capture. This means that these shear forces engender fluid flow vortices and induce fluid mixing that can displace weakly bound nonspecific species by tuning fluid shear forces at nanometer distances from the electrode surface. Thus, the unique features of ac-EHD-induced forces include (i) rapid ac-EHD-induced concentration of reaction products from the bulk solution into a confined volume and (ii) enhanced specificity resulting from the ability to tune the fluid force to shear away loosely bound, nonspecific species on the electrode surface.

Gold/silver nanoshells were employed as the plasmonic enhancer due to their tunable surface plasmon resonance, which can be optimized to the laser excitation to generate a maximum Raman-enhanced signal.^{17,18} Malachite green isothiocyanate (MGITC) was applied as the Raman reporter, which can provide a resonance Raman signal. A fluorescein isothiocyanate (FITC) conjugate with (3-aminopropyl)trimethoxysilane was further integrated into the SERS nanoshells for the fluorescence measurement. F-SERS nanotags with gold/silver nanoshells as the plasmonic enhancer and MGITC as Raman reporter were therefore prepared as represented in Supporting Information, Figure S2. Interestingly, these dual-functional nanotags encapsulated with the silica shell protect the Raman reporters as well as avoid any interference from the environment to the Raman signal. Thus, the silica shell represents a versatile method for the bioconjugation of the nanotags.¹⁹ The obtained F-SERS nanotags were characterized using transmission electron microscopy (TEM) analysis, extinction spectra, fluorescent spectra (FL), and SERS spectra as indicated in Figure 1b,c and Figure S2. The gold/silver shell with a diameter of ~ 55 nm and the coating of the silica shell with a thickness of around 20 nm can be observed clearly from the TEM image. Extinction spectra from bare

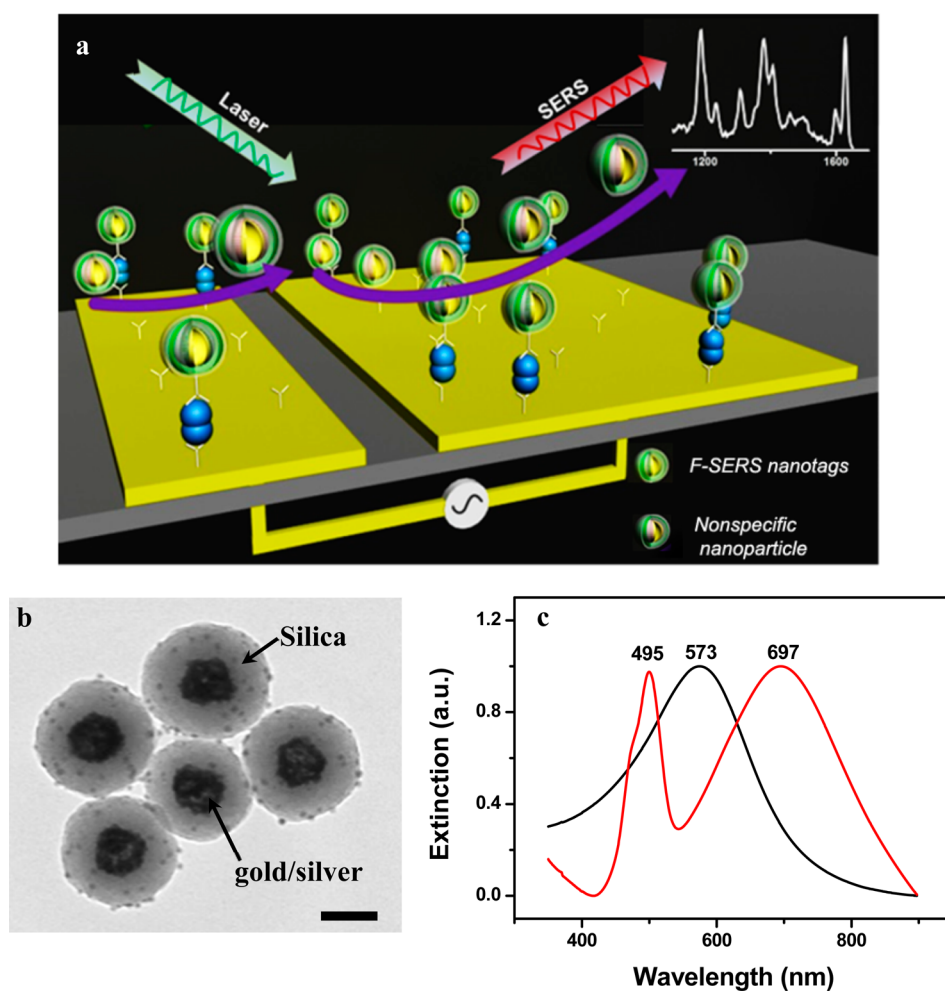


Figure 1. (a) Scheme for ac-EHD SERS immunoassay, (b) TEM image with a scale bar of 50 nm, and (c) extinction spectra of gold/silver nanoshells (black) and fluorophore-integrated gold/silver nanoshells.

gold/silver nanoshells (black line in Figure 1c) and F-SERS nanoshells (FITC-integrated silica-coated gold/silver shell with red line in Figure 1c) indicated that the localized surface plasmon resonance of gold/silver nanoshells shift from 573 to 697 nm upon the Raman reporter absorption and silica growth. The newly appearing peak at 495 nm (red line) is representative of the absorption of FITC, indicating the integration of FITC into the silica shell. FL spectrum (Figure S2c) of F-SERS nanotags further demonstrated the integration of FITC into the silica layer. Notably, FL of FITC is not quenched by plasmonic gold/silver nanoshells because of the gap between gold/silver nanoshells and FITC, which can facilitate simultaneous fluorescence and SERS measurements.

Comparison of ac-EHD SERS Immunoassay with Syringe Pump and Conventional SERS Immunoassay. Figure 2 represents the capture and detection of HER2 under an ac-EHD field. Briefly, the gold surface was coated with an anti-HER2 capture antibody using avidin–biotin chemistry. Serum samples containing target HER2 antigen were driven through the devices under an applied ac-EHD field. Subsequently, the captured HER2 antigen was

detected using detection-antibody-labeled F-SERS nanoshells under similar conditions of ac-EHD fluid flow.

Initially, to demonstrate the specificity of immunocapture, control experiments were performed using anti-HER2-functionalized devices (i) with and without target antigen, (ii) without detection antibody on SERS particles, and (iii) with and without ac-EHD force (see Figures S3 and S4 in the Supporting Information). As can be seen in Figure S4, ac-EHD-induced shear forces resulted in enhanced target capture. Negligible levels of nonspecific adsorption from detection antibody (e.g., without antigen) and F-SERS particles (e.g., without detection antibody) were observed (Figure S3). Further, more than 10-fold increase (Figure S4) in capture performance was observed under ac-EHD SERS immunoassay in comparison to devices without EHD (e.g., incubation of target and detection antibody for time periods similar to that under ac-EHD). These results indicate that ac-EHD-induced surface shear forces can potentially enhance the sensitivity and immunocapture in our devices.

To demonstrate the effectiveness of ac-EHD in enhancing SERS immunocapture, the capture

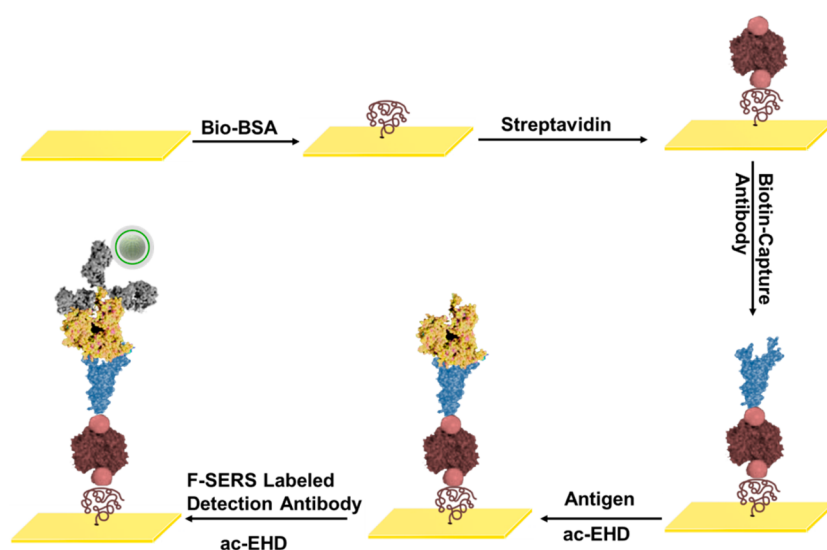


Figure 2. Schematic illustration of ac-EHD SERS immunoassay.

performance of the device under ac-EHD was compared with that obtained using a syringe pump and conventional SERS immunoassay (e.g., incubation of target and detection antibody). Simultaneously, to validate the levels of nonspecific adsorption associated with these immunoassays, a nonspecific nanoparticle (e.g., similar structure and different fingerprint) containing gold/silver nanoshells and 4-mercapto-3-nitrobenzoic acid (MNBA) as Raman reporters was spiked along with the F-SERS-labeled detection antibody (Figure 1a). For capture and detection of target protein, samples containing spiked HER2 protein (1 ng/mL) in serum were driven through anti-HER2-functionalized devices under an ac-EHD field of $f = 1$ kHz and $V_{pp} = 100$ mV and a flow rate of $7 \mu\text{L}/\text{min}$ (e.g., flow rate equal to that observed under ac-EHD) for syringe pump experiments (see Experimental Methods for more details). In the case of a conventional immunoassay, two 12 h incubation periods were followed for capture (e.g., 12 h for target antigen) and detection (e.g., 12 h for detection using F-SERS nanotags).

Figure 3a shows the false-color SERS images of F-SERS nanotags (1617 cm^{-1} from MGITC) and reference nanoparticles (1340 cm^{-1} from MNBA) for HER2 detection using different immunoassay platforms with the detection being performed at similar locations for each experiment. It was observed that ac-EHD-induced surface shear forces significantly enhanced the capture performance (e.g., SERS image of F-SERS nanotags) of the device in comparison to that using a syringe pump and/or conventional SERS immunoassay. Further, it was also observed that the level of nonspecific adsorption from the reference nanoparticle was also significantly reduced under ac-EHD. Raman intensity measurements (Figure 3b) obtained from these images suggest a 10- and 4-fold reduction in nonspecific adsorption under ac-EHD in comparison to that using a conventional

SERS immunoassay and syringe pump, respectively. These results indicate that ac-EHD-induced shear forces are highly effective in enhancing the capture performance (e.g., 4-fold enhancement) while also reducing any nonspecific adsorption from molecules present in biological fluids. Typical SERS spectra of F-SERS nanotags and reference nanoparticles are shown in Figure 3c, with the fingerprints from MGITC at 1180, 1390, and 1617 cm^{-1} being very clear in the three schemes. In case of ac-EHD, the fingerprint at 1340 cm^{-1} from reference nanoparticles in the case of ac-EHD SERS immunoassay was nearly inactive as evident from the negligible Raman signal. This further indicates that ac-EHD-induced surface shear forces were highly efficient in removing weakly bound SERS nanoparticles in comparison to syringe pump and conventional SERS immunoassay. The nonspecific binding from the conventional SERS immunoassay performed under static conditions results in high levels of adsorption of nonspecific nanoparticles or any associated proteins onto the surface, while in the case of the flow system, the increase in reaction kinetics reduced the nonspecific adsorption of nanoparticles on the surface, as indicated in the syringe pump and ac-EHD SERS immunoassay. Further, the use of ac-EHD significantly reduced the assay time from 24 h to 40 min due to the enhanced mass transport and concomitant flux mixing, which increased the number of sensor–target collisions.

Evaluation of the Performance of the ac-EHD SERS Assay. It is very important to evaluate the performance of the assay in a typical biological sample, such as serum. Therefore, sensitivity of the ac-EHD immunoassay was investigated with a microspectroscopic SERS scheme³ by performing the detection of HER2 antigen at different concentrations from 1 fg/mL to 1 ng/mL in human serum, which contains a high level of nontarget proteins. As indicated in Figure 4a, two parallel false-color SERS images from two different independent measurements using

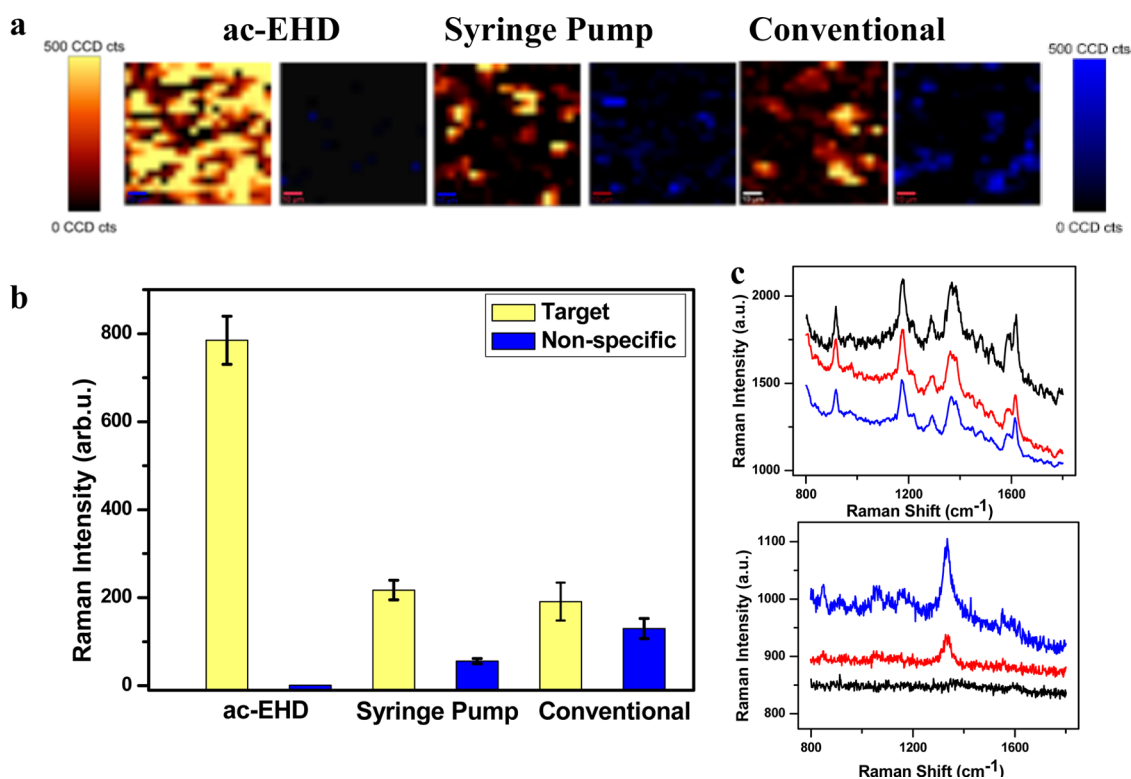


Figure 3. (a) False-color SERS images for ac-EHD immunoassay, syringe pump, and conventional SERS immunoassay with F-SERS nanotags (yellow) and reference nanoparticles (blue). Scale bar is 10 μm . (b) SERS intensity from positive and reference nanoparticles. (c) Typical SERS spectra for F-SERS and reference nanoparticles in ac-EHD SERS immunoassay (black), syringe pump immunoassay (red), and conventional SERS immunoassay (blue).

the integrated Raman intensity of MGITC at 1617 cm^{-1} at each concentration was reproducible and demonstrated an increase in SERS intensity with increasing HER2 concentration. Brighter images (*e.g.*, at higher concentrations) indicated the binding of more SERS-labeled detection antibodies on the surface and consequently generated a higher SERS signal. Scanning electron microscopy (SEM) analysis (Figure S5, Supporting Information) of the device at 10 pg/mL of HER2 corroborates these observations and also clearly indicates the structure of gold/silver nanoshells with silica coating.

Typical SERS spectra obtained at different concentrations are shown in Figure 4b, in which the distinct SERS peaks are seen more clearly. Notably, upon the increase of the concentration of the antigen resulted in an increase in SERS intensity. On the basis of SERS images at each concentration in the range of 1 fg/mL to 1 ng/mL , the concentration-dependent SERS intensity response curve was obtained (Figure 4c), in which the error bar represents the measurement of five different locations on three different electrodes, indicating that the developed ac-EHD immunoassay can determine HER2 at very low concentration in human serum with great reproducibility. The limit of detection for HER2 was determined to be 10 fg/mL , for which the signal is three times higher than the noise (0 fg/mL). We also noted that the signal for 1 fg/mL is similar to the background obtained without target antigen, further

demonstrating that the detection limit for this assay is 10 fg/mL with a dynamic range between 10 fg/mL and 100 pg/mL . Thus, this suggests that our approach is potentially capable of detecting protein biomarkers within the clinically relevant range.^{20–24}

Patient Sample Analysis. To investigate the diagnostic potential of this assay, the developed ac-EHD SERS immunoassay was applied for the analysis of HER2 in serum samples obtained from breast cancer patients. Six samples containing three HER2-positive and three HER2-negative patient serums were analyzed (see Experimental Methods for details). Control experiments were performed using serum samples obtained from healthy individuals. As can be seen in SERS images (Figure S6), higher levels of protein capture were observed in the case of HER2-positive patient samples compared to HER2-negative and the healthy sample, indicating the specific detection of the target HER2 antigen from patient samples by this assay. Typical SERS spectra from all nine patient samples showed clear and distinct peaks from SERS nanotags in the positive samples (Figure 5), further demonstrating the rapid and specific detection of the target in patient samples using ac-EHD SERS immunoassay. The approximate concentration ranges from these nine samples were calculated based on the average SERS intensity and fit with the calibration curve illustrated in Figure 4c. Table S1 (Supporting Information) represents the approximate concentration ranges for

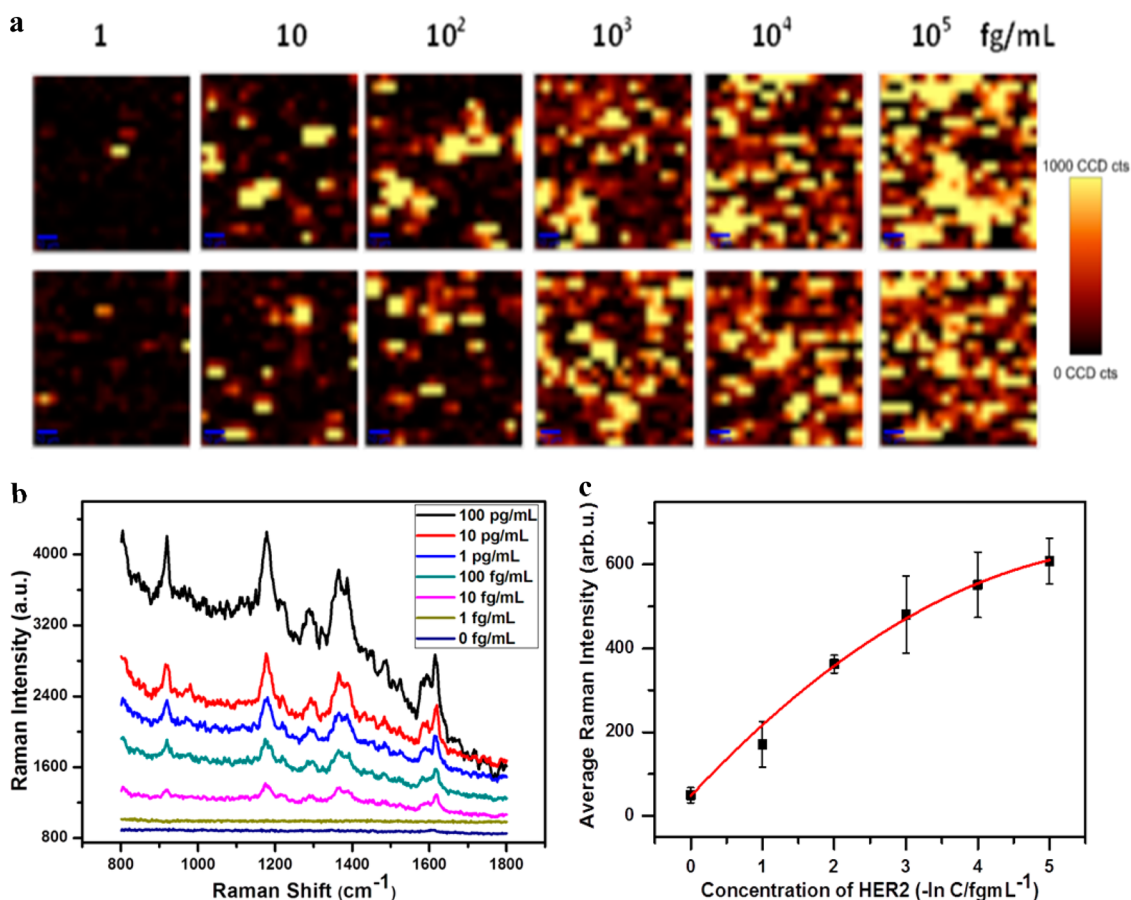


Figure 4. (a) False-color SERS images for HER2 detection at different concentrations in the range of 1 fg/mL to 100 pg/mL; scale bar is 10 μm . (b) Typical SERS spectra at each concentration and (c) concentration–intensity response curve.

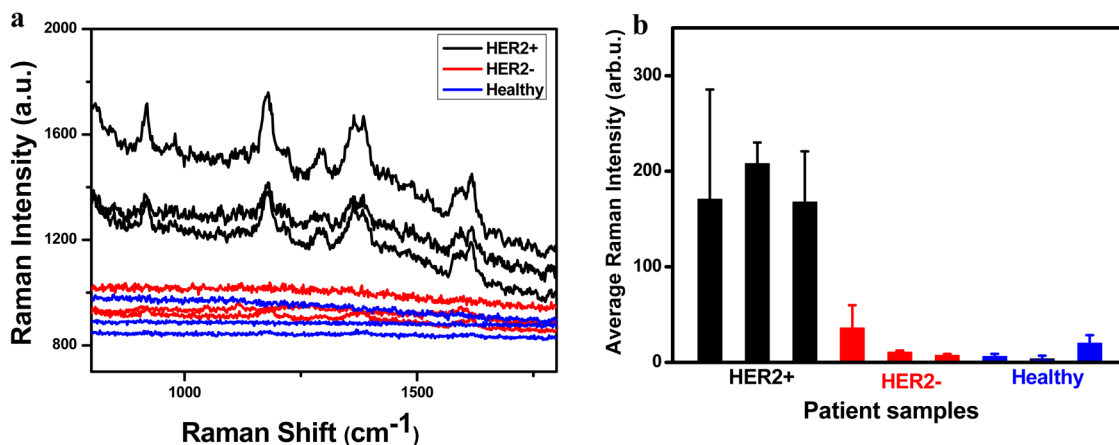


Figure 5. ac-EHD SERS immunoassay for HER2-positive (black), HER2-negative (red), and healthy patient (blue) analysis with (a) typical SERS spectra and (b) average Raman intensity for the patient samples.

these patient samples. The concentrations of HER2 obtained from these samples are well within the clinically relevant range.²⁵ It showed that serum from a HER2-positive patient produced a significantly higher SERS response compared to serum from HER2-negative and healthy individuals, further demonstrating that this platform can potentially be applied for the analysis of clinical samples.

CONCLUSION

In summary, a rapid and highly specific SERS immunoassay (ac-EHD immunoassay) was developed by using alternative current electrohydrodynamic force to significantly reduce the assay time and nonspecific binding during breast cancer biomarker detection. Rationally designed fluorescence-integrated gold/silver nanoshells were employed to monitor the capture

performance and associated nonspecific binding. It was found that the assay time with ac-EHD SERS immunoassay was shortened from 24 h to 40 min compared to the conventional SERS immunoassay with the nonspecific binding being 10 times lower than that of the conventional SERS immunoassay. We demonstrate that our approach is sensitive (10 fg/mL) and

can potentially detect concentrations of protein biomarkers from patient samples. We believe that this method can potentially contribute toward the development of SERS immunoassays with greater robustness and efficiency. Further, we also believe this approach could potentially find its relevance as a simple diagnostic tool.

EXPERIMENTAL METHODS

Materials. Malachite green isothiocyanate and fluorescein isothiocyanate were purchased from Invitrogen. Tetraethoxyorthosilicate (TEOS), (3-aminopropyl)trimethoxysilane (APTMS), ammonium hydroxide (30%), *N'*-(ethylcarbonimidoyl)-*N,N*-dimethylmonohydrochloride (EDC), *N*-hydroxysulfosuccinimide sodium salt, and 4-(2-hydroxyethyl)-1-piperazine ethanesulfonic acid (HEPES) were purchased from Sigma-Aldrich/Fluka. MNBA was prepared by breaking the disulfide bond in 5,5-dithiobis-(2-nitrobenzoic acid) with NaBH₄ as reducing agent before usage.

Monodispersed gold/silver nanoshells were prepared based on galvanic replacement as reported earlier by Xia and co-workers.^{17,26}

Biotinylated anti-HER2 polyclonal antibody, human recombinant HER2 antigen, and detection monoclonal antibody were purchased from R&D Systems. Biotin-BSA (bovine serum albumin) and streptavidin were procured from Invitrogen. PBS tablets were purchased from Astral Scientific.

Preparation of Silica-Encapsulated, Fluorescence-Integrated SERS Gold/Silver Nanoshells. FITC (10 mg/mL) in dimethylsulfoxide was reacted with 20 μ L of APTMS (100%) at room temperature in the dark for the conjugation of FITC to APTMS. Six milliliters of gold/silver nanoshells (with the optimized $\lambda_{\text{max}} = 600$ nm in water) was centrifuged and redispersed in 1.5 mL of ethanol. The colloid was then incubated overnight with 10 μ L of 1 mM MGITC to form a complete self-assembled monolayer on the particle surface. Silica-encapsulated, fluorescence-integrated SERS gold/silver nanoshells were prepared according to a previously reported method with slight modification.^{19,27} The thickness of the silica shell was adjusted by the amount of TEOS. After several hours of incubation, silica-coated F-SERS nanoparticles were centrifuged to remove the incubation solution, and the precipitate was redispersed into ethanol.

Biofunctionalization of F-SERS Nanoparticles. Silica-coated F-SERS nanoparticles were conjugated with antibodies after modification of the silica surface by a silane agent and standard EDC chemistry.³ Briefly, 1600 μ L of F-SERS nanoparticles (OD = 2.75) was first hydrolyzed with 268 μ L of ammonia (28%) under sonication at room temperature for 20 min. Afterward, the SERS nanoparticles were centrifuged once and redispersed into ethanol. Sixty-eight microliters of APTMS (0.5%) and 68 μ L of ammonia were added to the activated F-SERS nanoparticles and incubated at room temperature for 20 min under sonication. Amino-functionalized F-SERS clusters were further conjugated with 120 μ L of succinic anhydride to form carboxyl groups on the particles. F-SERS nanoparticles were centrifuged at 7000 rpm for 10 min and then washed in HEPES buffer. F-SERS nanoparticles were redispersed into HEPES twice and activated by EDC/*N*-hydroxysuccinimide (5 mg/1.5 mL for EDC and 3.77 mg/1.5 mL for NHS). Two micrograms of polyclonal antibody was added to the F-SERS nanoparticles and incubated at room temperature (25 °C) for 30 min and 4 °C overnight. F-SERS nanoparticles were then centrifuged at 7000 rpm for 10 min at 4 °C and redispersed in 0.5% BSA/PBS buffer prior to use in the bioassay. The as-prepared F-SERS labels are very stable and can be stored for several days before use.

Fabrication of the ac-EHD Microfluidic Platform. The ac-EHD microfluidic device contains three independent microfluidic channels, and each channel comprises 50 asymmetric planar electrode pairs. The narrow and wide electrodes of each asymmetric electrode pair in all three channels are connected to individual gold connecting pads that form the cathode and

anode, respectively. The device was fabricated using standard photolithography procedures and sandwiched between custom-built holders to introduce inlets and outlets for the reagents. Briefly, the gold patterns with widths of 25 and 100 μ m and spacing of 25 μ m were fabricated on a glass wafer using photolithography. The electrode patterns were designed in Layout Editor (L-Edit V15, Tanner Research Inc., CA) and printed on a chrome mask (5 in. \times 5 in.) obtained from Qingyi Precision Mask-Making (Shenzhen) Ltd., China. Pyrex glass wafers (4 in., 1 mm thick, double-side polished) were obtained from Bonda Technology, Singapore. The glass wafers were first cleaned in acetone and isopropyl alcohol (IPA) by sonication for 5 min in each case, rinsed with IPA, and dried with nitrogen gas. These were then coated with a negative photoresist (AZ nLOF 2070) at 3000 rpm for 30 s to obtain a \sim 7 μ m thick resist layer. The negative photo-resist-coated wafers then underwent a soft baking step at 110 °C for 6 min. These wafers were exposed to UV light (280 mJ/cm²) using the mask aligner (EVG 620, EV Group GmbH, Austria), and after a post-exposure bake step at 110 °C for 3 min, they were developed in AZ 726 developer solution for 3 min, followed by rinsing with deionized water (Millipore Pvt. Ltd., Australia) and drying under a flow of nitrogen gas. In this step, the unexposed negative photoresist was removed to realize the photoresist pattern. The wafers were then treated with oxygen plasma (60 W for 45 s) to remove any residual resist layer. The gold deposition (10 nm of titanium as adhesion layer followed by 200 nm of a gold layer) was carried out using a Temescal BJD-2000 e-beam evaporator. To obtain the gold patterns, we immersed these wafers in ethanol for the lift-off process. Finally, the wafers were diced into individual devices using the ADT-7100 dicing machine.

Each device was covered with polydimethylsiloxane (PDMS) containing three 400 μ m wide and 25 mm long channels with 1 mm diameter inlets and outlets. The PDMS molds were made by casting from SU8-2150 (MicroChem, U.S.A) master fabricated on a silicon wafer by following the standard photolithography process as per manufacturer's instructions. Briefly, the PDMS precursor was mixed with curing agent (10:1) (Sylgard 184 kit, Dow Corning), and after being degassed, it was poured on top of the SU-8 master followed by curing at 65 °C for 4 h. After this, the PDMS was released from the master, and 1 mm holes were punched into PDMS to open inlets and outlets.

Fabrication of the ac-EHD SERS Immunoassay. The bioassay platform was fabricated with several steps. Briefly, gold coated glass chips with three channels were first cleaned with Piranha solution and bonded to the PDMS containing the channels. Afterward, the device was sandwiched between custom-built holders and fixed into a microfluidic platform. Biotin-BSA at a concentration of 0.5 mg/mL was injected into each channel and left for the reaction at room temperature overnight. After each channel was washed several times using PBS buffer, 0.5 mg/mL streptavidin was reacted with biotin-BSA for 1 h. Biotinylated HER2 polyclonal antibody at a concentration of 10 μ g/mL was then employed to react with streptavidin at room temperature for 1 h, leading to the immobilization of the anti-HER2 antibody onto the gold surface.

Serum samples containing target protein were then driven through the device under an applied ac-EHD field strength of $f = 1$ kHz and $V_{\text{pp}} = 100$ mV, which was optimized previously^{14,15} to result in maximum capture due to the effective shear force manipulation that could simultaneously shear off nonspecific molecules while enhancing the number of capture antibody-target

and/or target–SERS detection antibody. Subsequently, the captured proteins were detected using a F-SERS-labeled detection antibody (HER2 monoclonal antibody) under similar conditions of ac-EHD-induced fluid flow. Serum samples (1 mL) of six breast cancer patients and three healthy individuals were obtained from Ventyx Wesley Research Institute Tissue Bank (Brisbane, Australia) and stored at $-80\text{ }^{\circ}\text{C}$ until further use. Immunohistochemical expression analysis suggested overexpression (3+: HER2(+)) and very low expression (1+: HER2(-)) of HER2 in these patient samples.

Syringe Pump and Conventional SERS Immunoassay. Instead of driving through samples containing HER2 antigen and/or F-SERS nanoparticles in the channels under an ac-EHD force, syringe pump experiment was performed at the flow rate of $7\text{ }\mu\text{L}/\text{min}$, which was equal to that obtained using ac-EHD flow. The equivalent flow rates were calculated based on the time required to flow 1 mL of sample under the ac-EHD field, and these flow rates were used for these experiments. Conventional SERS immunoassay was carried out with incubation of the HER2 antigen for 2 h and incubation of SERS labels for 12 h according to previous demonstrations.^{4,9}

Instruments. F-SERS nanoparticles were characterized by TEM (JEOL-2100) and UV–vis extinction spectroscopy (PerkinElmer, Lambda 35). SEM (Philips XL30) was applied to characterize the SERS particles on the gold surface to demonstrate the binding of F-SERS particles on the gold surface.

SERS spectra were recorded with a Witec alpha 300 R microspectrometer. The 632.8 nm line from a HeNe laser with a laser power of 4 mW on the sample was used for excitation of Raman scattering. The resolution for the Raman microspectrometer is 2 cm^{-1} . SERS images and spectra were obtained at 100 ms integration time, mapping an area of $80\text{ }\mu\text{m} \times 80\text{ }\mu\text{m}$ (20 pixel \times 20 pixel) using a $20\times$ microscope objective. A silicon wafer was used for calibration of the system by checking the laser power and focusing conditions based on the Raman intensity of the first-order photon peak of silicon at $\sim 520\text{ cm}^{-1}$. FL images were captured using a multichannel fluorescence microscope (Nikon Ti-U upright microscope, Melville, NY) and analyzed using image processing software (Nikon Ni-S elements, Basic Research).

Conflict of Interest: The authors declare no competing financial interest.

Acknowledgment. This work was supported by ARC DECRA (DE140101056). M.J.A.S. would like to thank ARC DECRA (DE120102503) for the financial support. We also would like to acknowledge the funding support from the National Breast Cancer Foundation of Australia to M.T. (CG-12-07) and ARC Discovery Project (DP140104006) to M.T. and M.J.A.S. These grants have significantly contributed to the environment to stimulate the research described here. We thank Yadveer Grewal for taking TEM and SEM images. The fabrication work and Raman measurement were conducted at Queensland node of the Australian National Fabrication Facility (Q-ANFF).

Supporting Information Available: Schematic illustration for preparing fluorescence-integrated silica-coated SERS nanoparticles; SERS and FL spectra of F-SERS nanotags; scheme for the device and fluorescence image, false-color SERS images for target antigen detection at 1 ng/mL with and without ac-EHD; FL and SERS for HER2 detection with 1 and 0 ng/mL, and SERS particles without detected antibody; ac-EHD SERS immunoassay for clinic sample detection with false-color SERS images and the approximate concentration ranges. The Supporting Information is available free of charge on the ACS Publications website at DOI: 10.1021/acsnano.5b01929.

REFERENCES AND NOTES

- Porter, M. D.; Lipert, R. J.; Siperko, L. M.; Wang, G.; Narayanan, R. SERS as a Bioassay Platform: Fundamentals, Design, and Applications. *Chem. Soc. Rev.* **2008**, *37*, 1001–1011.
- Schlücker, S. SERS Microscopy: Nanoparticle Probes and Biomedical Applications. *ChemPhysChem* **2009**, *10*, 1344–1354.

- Wang, Y.; Salehi, M.; Schütz, M.; Schlücker, S. Femtogram Detection of Cytokines in a Direct Dot-Blot Assay Using SERS Microspectroscopy and Hydrophilically Stabilized Au–Ag Nanoshells. *Chem. Commun.* **2014**, *50*, 2711–2714.
- Wang, G.; Park, H. Y.; Lipert, R. J.; Porter, M. D. Mixed Monolayers on Gold Nanoparticle Labels for Multiplexed Surface-Enhanced Raman Scattering Based Immunoassays. *Anal. Chem.* **2009**, *81*, 9643–9650.
- Wang, G.; Lipert, J.; Jain, M.; Kaur, S.; Chakraborty, S.; Torres, M. P.; Batra, S. K.; Brand, R. E.; Porter, M. D. Detection of the Potential Pancreatic Cancer Marker MUC4 in Serum Using Surface-Enhanced Raman Scattering. *Anal. Chem.* **2011**, *83*, 2554–2561.
- Faulds, K.; McKenzie, F.; Smith, W. E.; Graham, D. Quantitative Simultaneous Multianalyte Detection of DNA by Dual-Wavelength Surface-Enhanced Resonance Raman Scattering. *Angew. Chem., Int. Ed.* **2007**, *46*, 1829–1833.
- Cao, Y. C.; Jin, R. C.; Nam, J. M.; Thaxton, C. S.; Mirkin, C. A. Raman Dye-Labeled Nanoparticle Probes for Proteins. *J. Am. Chem. Soc.* **2003**, *125*, 14676–14677.
- Wang, G. F.; Driskell, J. D.; Porter, M. D.; Lipert, R. J. Control of Antigen Mass Transport via Capture Substrate Rotation: Binding Kinetics and Implications on Immunoassay Speed and Detection Limits. *Anal. Chem.* **2009**, *81*, 6175–6185.
- Wang, Y.; Salehi, M.; Schütz, M.; Rudi, K.; Schlücker, S. Microspectroscopic SERS Detection of Interleukin-6 with Rationally Designed Gold/Silver Nanoshells. *Analyst* **2013**, *138*, 1764–1771.
- Driskell, J. D.; Uhlenkamp, J. M.; Lipert, R. J.; Porter, M. D. Surface-Enhanced Raman Scattering Immunoassays Using a Rotated Capture Substrate. *Anal. Chem.* **2007**, *79*, 4141–4148.
- Penn, M. A.; Drake, D. M.; Driskell, J. D. Accelerated Surface-Enhanced Raman Spectroscopy (SERS)-Based Immunoassay on a Gold-Plated Membrane. *Anal. Chem.* **2013**, *85*, 8609–8617.
- Hucknall, A.; Rangarajan, S.; Chilkoti, A. In Pursuit of Zero: Polymer Brushes that Resist the Adsorption of Proteins. *Adv. Mater.* **2009**, *21*, 2441–2446.
- Blaszykowski, C.; Sheikh, S.; Thompson, M. Surface Chemistry To Minimize Fouling from Blood-Based Fluids. *Chem. Soc. Rev.* **2012**, *41*, 5599–5612.
- Shiddiky, M. J. A.; Vaidyanathan, R.; Rauf, S.; Tay, Z.; Trau, M. Molecular Nanoshearing: An Innovative Approach To Shear off Molecules with AC-Induced Nanoscopic Fluid Flow. *Sci. Rep.* **2014**, *4*, 3716.1–3716.6.
- Vaidyanathan, R.; Shiddiky, M. J. A.; Rauf, S.; Dray, E.; Tay, Z.; Trau, M. Tunable “Nano-Shearing”: A Physical Mechanism To Displace Nonspecific Cell Adhesion during Rare Cell Detection. *Anal. Chem.* **2014**, *86*, 2042–2049.
- Hunter, R. J. *Foundations of Colloidal Science*; Oxford University Press Inc.: New York, 1987.
- Sun, Y. G.; Mayers, B. T.; Xia, Y. N. Template-Engaged Replacement Reaction: A One-Step Approach to the Large-Scale Synthesis of Metal Nanostructures with Hollow Interiors. *Nano Lett.* **2002**, *2*, 481–485.
- Gellner, M.; Küstner, B.; Schlücker, S. Optical Properties and SERS Efficiency of Tunable Gold/Silver Nanoshells. *Vib. Spectrosc.* **2009**, *50*, 43–47.
- Yu, K. N.; Lee, S. M.; Han, J. Y.; Park, H.; Woo, M.; Noh, M. S.; Hwang, S. K.; Kwon, J. T.; Jin, H.; Kim, Y. K.; et al. Multiplex Targeting, Tracking, and Imaging of Apoptosis by Fluorescent Surface Enhanced Raman Spectroscopic Dots. *Bioconjugate Chem.* **2007**, *18*, 1155–1162.
- Wu, L.; Wang, Z.; Fan, K.; Zong, S.; Cui, Y. A SERS-Assisted 3D Barcode Chip for High-Throughput Biosensing. *Small* **2015**, *10*, 1002/sml.201403474.
- Gauchez, A. S.; Ravanel, N.; Villemain, D.; Brand, F. X.; Pasquier, D.; Payan, R.; Mousseau, M. Evaluation of a Manual ELISA Kit for Determination of HER2/neu in Serum of Breast Cancer Patients. *Anticancer Res.* **2008**, *28*, 3067–3073.
- Liu, D.; Huang, X.; Wang, Z.; Jin, A.; Sun, X.; Zhu, L.; Chen, X. Gold Nanoparticle-Based Activatable Probe for Sensing Ultralow Levels of Prostate-Specific Antigen. *ACS Nano* **2013**, *7*, 5568–5576.

23. Emaminejad, S.; Javanmard, M.; Gupta, C.; Chang, S.; Davis, R. W.; Howe, R. T. Tunable Control of Antibody Immobilization Using Electric Field. *Proc. Natl. Acad. Sci. U.S.A.* **2015**, *112*, 1995–1999.
24. Liu, X.; Dai, Q.; Austin, L.; Coutts, J.; Nowles, G.; Zou, J.; Chen, H.; Huo, Q. A One-Step Homogeneous Immunoassay for Cancer Biomarker Detection Using Gold Nanoparticle Probes Coupled with Dynamic Light Scattering. *J. Am. Chem. Soc.* **2008**, *130*, 2780–2782.
25. Moreno-Aspitia, A.; Hillman, D. W.; Dyar, S.; Tenner, K. S.; Gralow, J.; Kaufman, P. A.; Davidson, N. E.; Lafky, J. M.; Reinholz, M. M.; Lingle, W. L.; et al. Soluble Human Epidermal Growth Factor Receptor 2 (HER2) Levels in Patients with HER2-Positive Breast Cancer Receiving Chemotherapy with or without Trastuzumab: Results from North Central Cancer Treatment Group Adjuvant Trial N983. *Cancer* **2013**, *119*, 2675–2682.
26. Sun, Y.; Xia, Y. Increased Sensitivity of Surface Plasmon Resonance of Gold Nanoshells Compared to That of Gold Solid Colloids in Response to Environmental Changes. *Anal. Chem.* **2002**, *74*, 5297–5305.
27. Woo, M.; Lee, S.; Kim, G.; Baek, J.; Noh, M. S.; Kim, J. E.; Park, S. J.; Minai-Tehrani, A.; Park, S. C.; Seo, Y. T.; et al. Multiplex Immunoassay Using Fluorescent-Surface Enhanced Raman Spectroscopic Dots for the Detection of Bronchioalveolar Stem Cells in Murine Lung. *Anal. Chem.* **2009**, *81*, 1008–1015.